

A First-principles Prediction of Two-Dimensional Superconductivity in Pristine B₂C Single layer

Jun Dai, Zhenyu Li,* Jinlong Yang,* and Jianguo Hou

⁵ Hefei National Laboratory for Physical Science at the Microscale, University of Science and Technology of China, Hefei, Anhui 230026, China

^a Fax: 86-551-3603748; E-mail: zyl@ustc.edu.cn; jlyang@ustc.edu.cn.

¹⁰

Based on first-principles lattice dynamics and electron-phonon coupling calculations, B₂C sheet is predicted to be a two-dimensional (2D) phonon-mediated superconductor with a relatively high transition temperature (T_c). The electron-phonon coupling parameter calculated is 0.92, and it is mainly contributed by low frequency out-of-plane phonon modes and electronic states with a π character. When the Coulomb pseudopotential μ^* is set to 0.10, the estimated temperature T_c is 19.2 K. To be best of our knowledge, B₂C is the first pristine 2D superconductor with a T_c higher than the boiling point of liquid helium.

Superconductivity in layered materials has attracted numerous research interests since the discovery of high transition temperature (T_c) cuprate. MgB₂¹ and iron-based superconductors² are two recent examples of layered superconductors. Although the mechanism of superconductivity in cuprates and iron-based superconductors are still under debate, MgB₂ is known to be a conventional superconductor, which can be well interpreted in the framework of Bardeen-Cooper-Schrieffer (BCS) theory.³ Graphite intercalated compounds (GICs) is another type of layered BCS superconductor. Inspired by the relatively high T_c found in YbC₆ (6.5 K) and CaC₆ (11.5 K),⁴ research activities to the GICs family have been amplified. Different intercalated elements lead to different interlayer distance. Generally, the smaller the layer-layer separation, the larger the T_c.⁵ In BaC₆, the interlayer distance is so large that the superconductivity is almost suppressed. LiC₆ is an exception, in which the small intercalant-graphite distance results in an up-shift of the intercalant band above the Fermi level. As a result, superconductivity in LiC₆ is also suppressed.

Although superconductivity in layered structures have been extensively studied, little attention has been paid to two-dimensional (2D) single layers. Notice that 2D monolayer may have different superconducting properties than its corresponding layered bulk materials. For example, different from the non-superconducting bulk LiC₆, LiC₆ monolayer was predicted to have a T_c about 8 K.⁶ Using a rigid band approximation, Savini *et al.* also predicted *p*-doped graphane is an electron-phonon mediated superconductor with a T_c above 90 K.⁷ A pristine 2D superconducting system without doping is very attractive both fundamentally and practically. If existing, such a simple system will provide us an ideal platform to understand low-dimensional superconductivity, as

⁵⁵ MgB₂ did in three dimensions.^{3a}

To find a simple 2D superconductor, we first check the requirements for a material to be a BCS superconductor. In fact, most of the phonon mediated superconductors found after MgB₂, including boron-doped diamond,⁸ silicon,⁹ and silicon carbides,¹⁰ barium-doped silicon clathrates,¹¹ alkali-doped fullerenes,¹² GICs,⁴ and recent predicted *p*-doped graphane,⁷ can be grouped into “covalent-metal”.¹³ They are metallic yet have strong covalent bonds in their metallic states.

⁶⁵ As we know, within the framework of BCS theory, McMillan formula¹⁴ is used to predict T_c. It is related to the logarithmically averaged characteristic phonon frequency $\omega_{\text{in}}^{\text{ph}}$, the electron-phonon coupling parameter λ , and the Coulomb pseudopotential μ^* which describe the effective electron-electron repulsion.

$$T_c = \frac{\omega_{\text{in}}^{\text{ph}}}{1.20} \exp\left[\frac{-1.04(1+\lambda)}{\lambda - \mu^*(1+0.62\lambda)}\right] \quad (1)$$

Therefore, T_c will be maximized by increasing $\omega_{\text{in}}^{\text{ph}}$ and λ . Materials composed of light elements will have high frequency phonon modes, which may increase $\omega_{\text{in}}^{\text{ph}}$. Besides, λ is directly related to the electron-phonon coupling potential V and the electronic density of states (DOS) at the Fermi energy ($N(E_F)$), $\lambda = N(E_F)V$. Larger V and $N(E_F)$ will also lead to a higher T_c. With these rules in mind, searching for superconductors is still very challenging, because $\omega_{\text{in}}^{\text{ph}}$, V and $N(E_F)$ are strongly interwound. However, a rule of thumb is that phonon mediated superconductivity is more likely to appear in metallic systems with covalent bonds.

⁸⁵ In this paper, by using first-principles lattice dynamics and electron-phonon coupling (EPC) calculations, we predicted that B₂C single layer is a 2D intrinsic BCS superconductor. The calculated $\omega_{\text{in}}^{\text{ph}}$ and EPC parameter λ are 314.8 K and 0.92, respectively. They resulted a T_c of 19.2 K for μ^* equal to 0.10.

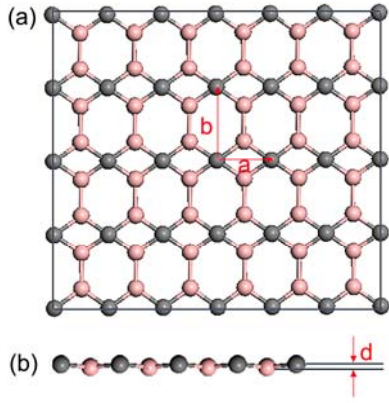
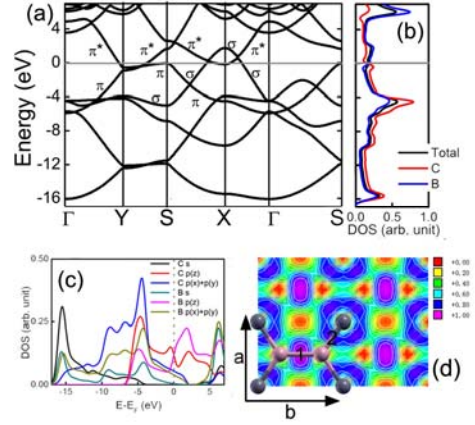


Fig. 1 (a) Top and (b) side view of optimized B₂C monolayer. Gray and pink spheres are carbon and boron atoms, respectively.



40

Fig. 2 (a) Electronic band structure and (b) density of states (DOS), (c) orbital-projected DOS of B₂C, (d) electron localization function of B₂C projected onto the B-plane. The total DOS in (b) is normalized to per atom for comparison. Γ (0.0, 0.0, 0.0), Y (0.5, 0.0, 0.0), S (0.5, 0.5, 0.0) and X (0.0, 0.5, 0.0) refer to the special points in the first Brouillon zone.

been synthesized, B₂C monolayer is predicted to be able to maintain its structural integrity up to 2000 K by Wu *et al.*²¹

The electronic band structure and DOS are shown in Fig. 2. B₂C sheet is metallic with three bands crossing the Fermi level (the bonding π band, the antibonding π^* band, and the bonding σ band). The presence of p_z -derived π and π^* band and $p_{x,y}$ -derived σ band at the Fermi level are similar to both MgB₂^{3b}, and GICs,^{24b} while the interlayer states in GICs are missing here due to the 2D character. In the atom-projected DOS, we can see both B and C contributions to the states at Fermi level. Orbital decomposed DOS (Fig. 2(c)) is obtained by using Löwdin population analysis. As expected from the band structure, the p_z orbital of C and B dominates at E_F , and there is also a smaller p_y (p_x) contribution from C and B character. $N(E_F)$ is 0.56 states/eV per 3-atom unit cell, close to that of MgB₂ (0.71 states/eV/cell)^{3a} but smaller than CaC₆ (1.59 states/eV/unitcell).^{24b}

In order to get a detail information about the bonding nature of B₂C sheet, we also performed electron localization function (ELF) analysis.²² ELF is related to the total electron density and its gradient, and it has been demonstrated to be very useful in terms of distinguishing different binding interactions.²³ ELF values ranges from 0 to 1 by definition. For perfectly localized electrons, such as participated in paired covalent bond, the corresponding ELF value should be close to 1. For a free electron gas, the ELF value should be smaller than 0.5. As shown in Fig. 2(d), there is a very strong covalent bond between B atoms, with an ELF value around 1. While the ELF value for B-C bonds is around 0.85, which also indicates a covalent bonding. In the area between two B-B bonds along the b direction, ELF values are approaching 0.5, suggesting delocalized electrons.

Now, we can see that that B₂C meets the essential requirements for a BCS-type superconductor, namely, being metallic and covalent bonding. It is thus desirable to directly check its phonon dispersion and electron-phonon coupling property. The phonon band structure and DOS are shown in Fig. 3. First, we are confirmed that B₂C is dynamically stable,

Electronic structure calculations and geometrical optimizations are performed using density-functional theory (DFT)¹⁵ within local-density approximation (LDA).¹⁶ Such a protocol has been successfully applied in similar systems, such as boron-doped diamond.¹⁷ A vacuum space around 20 Å along the direction perpendicular to the B₂C sheet is used in order to eliminate the interlayer interaction generated by periodic boundary condition. The electron-ion interaction is described by ultrasoft pseudopotentials,¹⁸ and a energy cutoff of 60 Ry is used. EPC calculations are carried out using density-functional perturbation theory with linear response.¹⁹

The k -point integration for geometrical optimization, construction of the induced charge density, and calculations of dynamical matrix is performed over a $36 \times 36 \times 1$ Monkhorst-Pack grid,²⁰ and a finer $72 \times 72 \times 1$ grid is used in the phonon linewidth calculations, where the convergence in the k -point sampling is more difficult. The dynamical matrix and phonon linewidth are computed on a $12 \times 12 \times 1$ q -point mesh, and a Fourier interpolation is used to obtain complete phonon dispersions. A smearing of 0.02 Ry is used to speed up convergence. The convergence of phonon dispersion with respect to energy cutoff, k -points sampling and smearing has been carefully checked, the choice of 60 Ry, $36 \times 36 \times 1$ grid and a smearing of 0.02 Ry gives convergence within about 2% on phonon modes at Γ and X and less than 1 mRy on the total energy.

As shown in Fig. 1, B₂C monolayer is composed of rectangular B₂C building blocks. In the a direction, neighboring rectangular B₂C units share two common boron atoms. In the b direction, neighboring B₂C units are connected via B-B covalent bonds. By this way, it forms a sheet composed of hexagons and rhombuses. The optimized lattice constants are $a=2.552$ Å, and $b=3.392$ Å. The bond length of B-B and B-C are 1.667 Å and 1.541 Å, respectively. The B₂C monolayer is slightly corrugated with the boron layer and carbon layer separated by ~ 0.032 Å. Although it has not yet

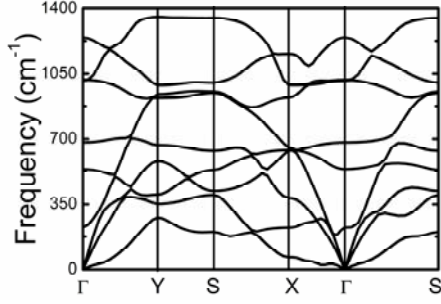


Fig. 3 Phonon band structure of B₂C sheet.

with a well-converged phonon band structure and no structural instability. Very recently, Xiang et al. have found another low-energy B₂C structure.²⁴ Optimized with the computational method adopted in this study, their structure is 44.7 meV per atom lower in energy than the current structure. However, we emphasize that, provided it is dynamically stable, even a metastable structure should be able to obtain experimentally in principle.

Based on group theory, the 9 modes at Γ points can be decomposed as:

$$\Gamma_{\text{vib}} = 3A_1(\text{IR} + \text{R}) + 3B_1(\text{IR} + \text{R}) + A_2(\text{R}) + 2B_2(\text{IR} + \text{R})$$

The calculated frequency of the highest optical mode at Γ is 1243 cm⁻¹, which is corresponding to a B-B stretching mode. Such a high frequency is consistent with the strong covalent bonding suggested by ELF. This mode is active in both Raman and IR spectroscopy.

We then use the Eliashberg function $\alpha^2F(\omega)$ to analyze contribution of each phonon mode to the electron-phonon coupling constant:

$$\alpha^2F(\omega) = \frac{1}{2N_q} \sum_{q\nu} \lambda_{q\nu} \omega_{q\nu} \delta(\omega - \omega_{q\nu}) \quad (2)$$

where N_q is the number of q points used, and $\lambda_{q\nu}$ is the electron-phonon interaction for a phonon ν with momentum q , which can be written as:

$$\lambda_{q\nu} = \frac{4}{\omega_{q\nu} N(0) N_k} \sum_{k,n,m} |g_{kn,k+qm}^\nu|^2 \delta(\epsilon_{kn}) \delta(\delta_{k+qm}) \quad (3)$$

Here $N(0)$ is the density of states at Fermi energy, and N_k is the number of k points, the matrix element is:

$$g_{kn,k+qm}^\nu = \frac{\langle kn | \delta V / \delta \mathbf{u}_{q\nu} | k + qm \rangle}{\sqrt{2\omega_{q\nu}}} \quad (4)$$

where $\mathbf{u}_{q\nu}$ is the amplitude of the displacement of the phonon and V is the Kohn-Sham potential.

We show in the Fig. 4 the Eliashberg function $\alpha^2F(\omega)$, the integral $\lambda(\omega) = 2 \int d\omega' \alpha^2F(\omega') / \omega'$ and the displacement decomposed partial phonon DOS of B and C in in-plane (xy , parallel to the B₂C sheet) and out-of-plane (z , perpendicular to the B₂C sheet) contributions. The partial phonon DOS for atom a is defined as: $\rho_a(\omega) = \sum_q \sum_{j=1}^{3N} |e_a(q, j)|^2 \delta[\omega - \omega(q, j)]$, where N is the total number of atoms, q is the phonon

momentum, j labels the phonon branch, $e_a(q, j)$ is the phonon displacement vector for atom a , and $\omega(q, j)$ is the phonon frequency. In MgB₂ and GICs, due to the weak bonding

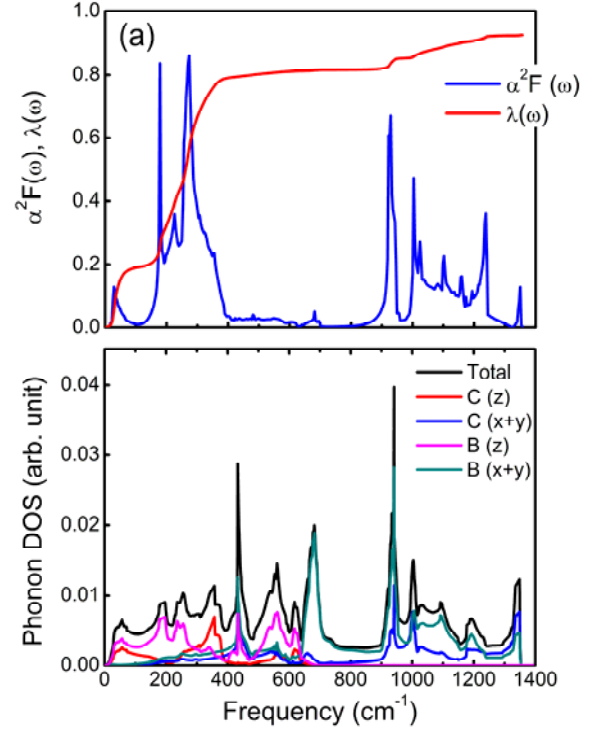


Fig. 4 (a) Eliashberg spectral function $\alpha^2F(\omega)$ and integrated electron-phonon coupling $\lambda(\omega)$ for B₂C sheet. (b) Total phonon DOS and partial phonon DOS projected on selected vibrations.

between Mg²⁺ (alkali atom) and B plane (graphene), the decomposed phonon DOS is well separated in energy for different elements.²⁵ In B₂C sheet, the strong bonding between B and C make phonon DOS of B and C largely intertwined except for the B out-of-plane mode around 200 cm⁻¹ and B in-plane modes around 700 and 1100 cm⁻¹.

Different from MgB₂ in which the electron-phonon interaction almost comes from the E_{2g} phonon entirely, and that in GICs where symmetry forbids the coupling between π -states and the softer out-of-plane vibrations, coupling with out-of-plane vibrations is significantly promoted in B₂C sheet. Besides, vibrations in the range from 200 to 400 cm⁻¹ contribute the largest part of the total λ , namely about 0.5 of 0.92. Most of this part of the coupling is from out-of-plane modes, especially, in the region near 200 and 350 cm⁻¹. The strong coupling of electrons with out-plane modes is presumedly due to the dominating π character, and the coupling of π electron with out-of-plane modes in B₂C sheet is symmetry allowed. $\omega_{\text{in}}^{\text{ph}}$ of B₂C is 314.8 K, larger than that of CaC₆ (286.6 K)^{24b}, but much smaller than that of MgB₂ (~ 700 K)^{3a,3b}. The typical μ^* is in the range 0.10-0.15, thus, by using the McMillan formula, the calculated T_c is in the range of 19.2 ($\mu^*=0.10$) to 14.3 ($\mu^*=0.15$), indicating B₂C sheet is an intrinsic BCS-type superconductor with a relative

high T_c .

In summary, we have carried out a first-principles study on the 2D B_2C sheet, and the intrinsic phonon mediated superconductivity is predicted with T_c ranges in 14.3-19.2 K. The low frequency out-of-plane phonon modes contribute to most of the coupling. The intrinsic superconductivity in B_2C may offer a better platform to investigate the superconductivity in low dimensional systems, and B_2C is also a good starting point to obtain high T_c in 2D systems. T_c is expected to increase if more σ bands are shifted to the Fermi level, since σ states are easier to couple with high-frequency phonon modes.

Acknowledgements

This work is partially supported by NSFC (20933006, 91021004, and 21173202), by CUSF, by the National Key Basic Research Program (2011CB921404), by the Fundamental Research Funds for the Central Universities, by USTCSCC, SCCAS, and Shanghai Supercomputer Center.

Notes and references

- 1 J. Nagamatsu, N. Nakagawa, T. Muranaka, and J. Akimitsu, *Nature*, 2001, **410**, 63-64.
- 2 Y. Kamihara, T. Watanabe, M. Hirano, and H. Hosono, *J. Am. Chem. Soc.*, 2008, **130**, 3296-3297.
- 3 (a) J. An and W. Pickett, *Phys. Rev. Lett.*, 2001, **86**, 4366. (b) J. Kortus, I. Mazin, K. Belashchenko, V. Antropov, and L. Boyer, *Phys. Rev. Lett.* 2001, **86**, 4656. (c) K. Bohnen, R. Hield and B. Renker, *Phys. Rev. Lett.*, 2001, **86**, 5771. (d) T. Yildirim, O. Gülseren, J. Lynn, C. Brown, T. Udovic, Q. Huang, M. Rogado, K. Regan, M. Hayward, J. Slusky, T. He, M. Hass, P. Khalifah, K. Inumaru and R. Cava, *Phys. Rev. Lett.*, 2001, **87**, 037001. (e) Y. Kong, O. Dolgov, O. Jepsen and O. Andersen, *Phys. Rev. B*, 2001, **64**, 020501.
- 4 (a) T. Weller, M. Ellerby, S. Saxema, R. Smith and N. Skipper, *Nature Phys.*, 2005, **1**, 39-41. (b) E. Emery, C. Hérold, M. d' Astuto, V. Garcia, Ch. Bellin, J. Marêché, P. Lagrange and G. Loupías, *Phys. Rev. Lett.*, 2005, **95**, 087003.
- 5 (a) J. Kim, L. Boeri, J. O' Brien, F. Razavi and R. Kremer, *Phys. Rev. Lett.*, 2007, **99**, 027001. (b) A. Gauzzi, S. Takashima, N. Takeshita, C. Terakura, H. Takagi, N. Emery, C. Hérold, P. Lagrange and G. Loupías, *Phys. Rev. Lett.*, 2007, **98**, 067002. (c) R. Smith, A. Kusmartseva, Y. Ko, S. Saxena, A. Akrap, L. Forró, M. Laad, T. Weller, M. Ellerby and N. Skipper, *Phys. Rev. B*, 2006, **74**, 024505.
- 6 G. Profeta, M. Calandra and F. Mauri, *arXiv e-print: arXiv:1105.3736v1*, 2011.
- 7 G. Savini, A. Ferrari, F. Giustino, *Phys. Rev. Lett.*, 2010, **105**, 037002.
- 8 E. A. Ekimov, V. A. Sidorov, E. D. Bauer, N. N. Mel'nik, N. J. Curro, J. D. Thompson and S. M. Stishov, *Nature*, 2004, **428**, 542-545.
- 9 E. Bustarret, C. Marcenat, P. Achatz, J. Kapčmarčík, F. Lévy, A. Huxley, L. Ortéga, E. Bourgeois, X. Blase, D. Débarre and J. Boulmer, *Nature*, 2006, **444**, 465-468.
- 10 (a) Z. Ren, J. Kato, T. Muranaka, J. Akimitsu, M. Kriener and Y. Maeno, *J. Phys. Soc. Jpn.*, 2007, **76**, 103710. (b) M. Kriener, Y. Maeno, T. Oguchi, Z. Ren, J. Kato, T. Muranaka and Akimitsu, J.; *Phys. Rev. B*, 2008, **78**, 024517.
- 11 (a) H. Kawaji, H. O. Horie, S. Yamanaka and M. Ishikawa, *Phys. Rev. Lett.*, 1995, **74**, 1427. (b) K. Tanigaki, T. Shimizu, K. M. Itoh, J. Teraoka, Y. Moritomo and S. Yamanaka, *Nature Mater.*, 2003, **2**, 653-655.
- 12 (a) A. F. Heberd, M. J. Rosseinsky, R. C. Haddon, D. W. Murphy and S. H. Glarum, *Nature*, 1991, **350**, 600-601. (b) C. M. Varma, J. Zaanen and K. Raghavachari, *Science*, 1991, **254**, 989-992.
- 13 X. Blase, E. Bustarret, C. Chapelier, T. Klein and C. Marcenat, *Nature Mater.*, 2009, **8**, 375-382.
- 14 W. L. McMillan, *Phys. Rev.* 1968, **167**, 331.
- 15 (a) P. Hohenberg and W. Kohn, *Phys. Rev.*, 1964, **136**, B864. (b) W. Kohn and L. J. Sham, *Phys. Rev.*, 1965, **140**, A1133.
- 16 (a) D. M. Ceperley and B. J. Alder, *Phys. Rev. Lett.*, 1980, **45**, 556. (b) J. P. Perdew and A. Zunger, *Phys. Rev. B*, 1981, **23**, 5048.
- 17 (a) X. Blase, Ch. Adessi and D. Connétable, *Phys. Rev. Lett.*, 2004, **93**, 237004. (b) H. J. Xiang, Z. Li, J. Yang, J. Hou and Q. Zhu, *Phys. Rev. B*, 2004, **70**, 212504.
- 18 P. Vanderbilt, *Phys. Rev. B*, 1990, **41**, 7892.
- 19 P. Giannozzi, S. Baroni, N. Bonini, M. Calandra, R. Car, C. Cavazzoni, D. Ceresoli, G. L. Chiarotti, M. Cococcioni, I. Dabo, A. D. Corso, S. de Gironcoli, S. Fabris, G. Fratesi and R. Gebauer, *J. Phys. Condens. Matter*, 2009, **21**, 395502.
- 20 H. J. Monkhorst and J. D. Pack, *Phys. Rev. B*, 1995, **13**, 5188.
- 21 X. Wu, Y. Pei and X. C. Zeng, *Nano. Lett.*, 2009, **9**, 1577-1582.
- 22 A. Savin, R. Nesper, S. Wenger and T. F. Fäslér, *Angew. Chem. Int. Ed.*, 1997, **36**, 1808-1832.
- 23 Z. Li, J. Yang, J. G. Hou and Q. Zhu, *Angew. Chem. Int. Ed.*, 2004, **43**, 6479-6482.
- 24 X. Luo, J. Yang, H. Liu, X. Wu, Y. Wang, Y. Ma, S.-H. Wei, X. Gong, and H. Xiang, *J. Am. Chem. Soc.*, 2011, **133**, 16285-16290. Based on our calculations, the B_2C structure reported in this reference with the lowest energy has a transition temperature of about 5 K.
- 25 (a) R. Osborn, E. A. Goremychkin, A. I. Kolesnikov and D. G. Hinks, *Phys. Rev. Lett.* 2001, **87**, 017005. (b) M. Calandra and F. Mauri, *Phys. Rev. Lett.* 2005, **95**, 237002.